A.V. SACHENKO,[1] V.P. KOSTYLYOV,[1] V.G. LITOVCHENKO,[1] V.G. POPOV,[1]
B.M. ROMANYUK,[1] V.V. CHERNENKO,[1] V.M. NASEKA,[1] T.V. SLUSAR,[2]
S.I. KYRYLOVA,[1] F.F. KOMAROV[3]

[1]V.E. Lashkaryov Institute of Semiconductor Physics, Nat. Acad. of Sci. of Ukraine
(41, Nauky Ave., Kyiv 03028, Ukraine; e-mail: vglytovchenko@gmail.com)
[2]National Aviation University
(1, Cosmonaut Komarov Ave., Kyiv 03058, Ukraine)
[3]A.N. Sevchenko Institute for Applied Physical Problems, Belarusian State University
(7, Kurchatov Str., Minsk 220108, Belarus; e-mail: kff@tut.by)

PACS 72.20.Jv

RECOMBINATION CHARACTERISTICS OF SINGLE-CRYSTALLINE SILICON WAFERS WITH A DAMAGED NEAR-SURFACE LAYER

Spectral dependences of the small-signal surface photovoltage, $V_f(\lambda)$, with a region of short-wave recession have been studied experimentally and theoretically. The dependences $V_f(\lambda)$ are shown to enable important information concerning a modification of surface and bulk recombination properties of the photosensitive silicon material in the short-wave spectral range to be obtained experimentally with the use of a nondestructive technique. In particular, the formation of a damaged near-surface layer owing to the Fe implantation is found to bring about a significant decrease in the diffusion length (i.e. the lifetime) in the implanted layer and an increase of the effective surface recombination rate on the illuminated surface.

Keywords: surface photovoltage, surface recombination, silicon

1. Introduction

The recombination activity of single- and polycrystalline silicon is one of its main characteristics. It has the bulk and surface components. In the bulk, the recombination activity is characterized by the diffusion length L or the lifetime of nonequilibrium minority charge carriers. The problem of fabricating a silicon material with a large L-value is very important for its application while manufacturing the solar energy photoconverters. The magnitude of L is governed by both purity and structural perfection of the initial material, on the one hand, and the influence of technological procedures–annealing, doping, and so forth–used at manufacturing the photoconverters or other devices, on the other hand. One of the main methods used for the determination of the parameter L and classed as an international standard is the measurement of spectral dependences of the surface photovoltage V_f [1–6]. Actually, the spectral range, where the influence of L-value on the spectral dependence of V_f manifests itself, includes the red and near infra-red intervals.

As was shown in work [7], the spectra of V_f are also sensitive to the recombination parameters of silicon in the near-surface region of the specimen. Those parameters are responsible for the emergence of a short-wave recession in the violet and blue intervals of V_f-spectra. In this work, the V_f-spectra were examined in detail – in particular, their short-wave region – and the theoretical approaches to the analysis of the obtained results were developed.

2. Experimental Technique and Specimens

Surface photovoltage was measured with the use of the capacitance method. The registered signal was processed in a computer for its normalization to the number of light quanta incident on the specimen.

As experimental specimens, standard wafers of single-crystalline silicon KDB-10 (100) grown by the Czochralski method were used. The wafers were either not subjected to any additional treatments or chemically etched in the CP-4 mixture. Some specimens were implanted with ions of the recombination-active iron impurity (an energy of 130 keV and exposure doses of 2 and 18 $\mu C/cm^2$) and annealed at a temperature of 750 °C for 30 min in an argon atmosphere. To clean the bulk of specimens from impurities, we used the method of gettering with an aluminum layer coated on the rear wafers surface.

The equilibrium surface band bending in the examined specimens was determined with the help of the technique described in work [8] using a flash lamp. The surface band bending was measured for two specimens, unethched and etched in HF, and the values of 0.22 and 0.26 V, respectively, were obtained, which testifies to the presence of a depleted space charge region (SCR).

3. Analysis of the Spectral Dependence of Surface Photovoltage

In typical spectral dependences of the small-signal surface photovoltage $V_f(\lambda)$, where λ is the illumination wavelength, which are registered for silicon specimens fabricated by cutting a semiconductor ingot into wafers and by etching their surfaces in an etching solution, which removes – at least partially – a mechanically damaged layer, the regions of short-wave recession are usually observed [7]. In order to determine the diffusion lengths L from the spectral dependences of law-signal photovoltage usually the methods based on analysis of the half-magnitude point in the dependence $V_f(\lambda)$ or the cut-off point coordinate on the abscissa axis for the dependence $V_f^{-1}(\alpha^{-1})$ are used.

In order to determine the diffusion length L from the spectral dependences of the small-signal photovoltage, the normalized spectral dependence $V_f/V_{f\max} = \alpha L/(\alpha L+1)$ is considered. Alternatively, the ideologically closest methods, which are based on the analysis of the half-magnitude point in the dependence $V_f(\lambda)$ or the cutoff-point coordinate on the abscissa axis for the dependence $V_f^{-1}(\alpha^{-1})$, are applied. However, they are suitable well when the relation $d > 2L$ is obeyed, where d is the specimen thickness. If the latter is comparable or smaller that the diffusion length, the methods mentioned above do not allow the parameter L to be determined correctly [5, 6].

We note that, while explaining the experimental results obtained for surface-sensitive photoeffects in semiconductors (e.g., photoconductivity and surface photovoltage), the surface recombination rate S was first used as an independent parameter. It was sufficient for the short-wave recession in the spectral dependences of photoconductivity to be explained by the influence of surface recombination. However, in the case of the surface photovoltage, the situation becomes complicated. For the short-wave recession to be explained, it is necessary to introduce the effective rate of surface recombination S_{eff}, which is a function of a number of parameters. In particular, besides the surface band bending, these are also the parameters of surface recombination levels, as well as the illumination wavelength λ. The latter governs the depth, at which electron-hole pairs are generated in a semiconductor. The general expressions for the parameter S_{eff} are given and analyzed in [9, 10] and will be analyzed below in detail. Note, in particular, that if the quantity S_{eff} does not depend on λ, there is no short-wave recession in the spectral dependences of the surface photovoltage.

In the subsequent analysis, we assume that the relation $d \geq 2L$ is satisfied, i.e. the specimen is thick. Let us examine the origin of short-wave recession for $V_f(\lambda)$ under those conditions and determine which parameters can be obtained if this recession does take place. It should be noted that the dependence $V_f(\lambda)$ for the small-signal surface photovoltage has the following general form for the hole semiconductor [9,10]:

$$V_f(\lambda) = \frac{I}{p_0}\frac{kT}{q}\frac{(\kappa+1)e^{y_s}-1}{(S_{\text{ef}}+D/L)(1+(\kappa+1)e^{y_s-2u_b})}\times$$
$$\times\frac{\alpha(\lambda)L}{1+\alpha(\lambda)L}, \tag{1}$$

Therefore, the short-wave recession region is absent if the magnitude of effective surface recombination rate on the illuminated surface, S_{eff}, does not depend on the light absorption coefficient α, i.e. on the illumination wavelength λ. In formula (1), the following notations are used: κ is a dimensionless coefficient describing the surface charge redistribution at the illumination, k the Boltzmann constant, T the absolute temperature, q the electron charge, I the monochromatic illumination intensity, p_0 the equilibrium concentration of holes in the bulk, y_s the dimensionless equilibrium band bending at the illuminated surface, $y_b = \ln(p_0/n_i)$ the Fermi potential reckoned from the middle of the energy gap, and D is the diffusion coefficient for minority charge carriers.

In the case of enriching band bending at the p-type semiconductor surface, i.e. when $y_s < 0$, the value of $V_f(\lambda)$ is negative, being the smallest by the absolute value. When the depleting band bending increases, the value of $V_f(\lambda)$ grows exponentially as the value of y_s increases, whereas, in the case of the inverted band bending, i.e. when $y_s > 2u_b$, the magnitude of photovoltage $V_f(\lambda)$ is saturated. The ratio between the $V_f(\lambda)$-values at the inverted band bending and in a vicinity of the flat bands is approximately equal to $(p_0/n_i)^2$, where n_i is the concentration of intrinsic charge carriers. In silicon at room temperature and $p_0 = 10^{15}$ cm^{-3}, this ratio is about 10^{10}. This means that, at inverted band bendings, the small-signal photovoltage can be realized only if the illumination intensities are very low. For instance, in silicon with $p_0 = 10^{15}$ cm^{-3} and $S = 10^5$ cm/s at inverted band bendings, the condition for the small-signal photovoltage to be obtained is obeyed if $I < 10^{10}$ cm^{-2}s^{-1}. This requirement becomes substantially weaker if we change from the inverted band bendings to the depleting ones and if the latter decrease. In the indicated cases, the surface photovoltage is small-signal at $I \gg 10^{10}$ cm^{-2}s^{-1} as well.

As was marked above, for the short-wave recession to take place, it is necessary that the effective rate of surface recombination on the illuminated surface, $S_{\rm eff}$, should depend on the illumination wavelength λ and increase, as λ diminishes. One of the mechanisms responsible for such a dependence $S_{\rm eff}(\lambda)$ is described in work [10]. It is the case where the Fermi quasilevel for minority charge carriers in the near-surface SCR is not constant. The specified mechanism consists in that the effective rate of recombination on the surface substantially depends on the site of the electron-hole pair generation in the case where its value is high enough. In particular, when the light absorption is rather weak – i.e. if $\alpha\omega \ll 1$, where ω is the thickness of the near-surface SCR, so that the excess charge carriers are generated beyond the SCR – the effective surface recombination rate is driven by the rate of nonequilibrium charge carrier supply to the surface, i.e. by the diffusion rate. If absorption is so strong that all excess charge carriers are generated in the SCR, i.e. if $\alpha\omega \gg 1$, the effective rate of surface recombination on the illuminated surface grows and is determined by the recombination activity of the surface itself characterized by the recombination rate S_0.

In the case where a depleting band bending takes place at the surface, it is the minority charge carriers that are responsible for the process of excess electron-hole pair delivery to the surface. In this case, the value $S_{\rm eff}(\lambda)$ is determined by the expression [10]:

$$S_{\rm eff}(\lambda) = \frac{S_0 S_p(\lambda)}{S_0 + S_p(\lambda)}, \qquad (2)$$

where

$$S_p(\lambda) = \frac{D}{\int_0^\omega \exp[-\alpha(\lambda)x + y_s(1 - x/\omega)^2]dx},$$

where S_0 is the effective rate of surface recombination under the surface generation of electron-hole pairs, and D is the diffusion coefficient for the minority charge carriers.

The value $S_p(\lambda)$ describes the rate of minority charge carrier supply to the surface as a function of the site where electron-hole pairs are generated. It is minimal, when electron-hole pairs are generated beyond the SCR and is very large if the generation occurs close to the surface. Hence, expression (2) describes a situation where the effective rate of surface recombination $S_{\rm eff}$ can be restricted by the supply of minority charge carriers to the surface.

In the SCR, the minority charge carriers – in our case, these are electrons – are accelerated toward the surface. Therefore, if excess electron-hole pairs are generated beyond the SCR, the value of $S_p^{\rm min}$ equals, by the order of magnitude, D/L_D, where L_D is the Debye screening length. It happens because, in this case, the total time of diffusion of electrons through the SCR becomes close to the time of their passage through an SCR of the thickness L_D, in which the field does not affect substantially their velocity. Let us evaluate the quantity D/L_D in the case where the doping level of the semiconductor material is 10^{15} cm^{-3}. We obtain that $L_D \approx 10^{-5}$ cm and $S_p^5 \approx 3 \times 10^6$ cm/s. Hence, in this case, for the value $S_{\rm eff}(\lambda)$ to grow when changing from the regime of light absorption in the bulk to that at the surface under the linear excitation mode, it is necessary that the condition $S_0 > 10^6$ cm/s be satisfied.

In Fig. 1, the dependences $S_{\rm eff}(\lambda)$ calculated by formula (2) for p-silicon with a doping level of 10^{15} cm^{-3} are exhibited. The curves are parametrized by the value of S_0. The figure demonstrates that the larger the S_0-value, the larger is its difference from $S_{\rm eff}^{\rm min}$, the latter being realized when light generates electron-hole pairs beyond the SCR. However, this value is smaller than that of $S_p^{\rm min}$. Only if $S_0 \gg S_p^{\rm min}$, the values of $S_{\rm eff}^{\rm min}$ and $S_p^{\rm min}$ come closer to each other.

Note that the dependence $S_{\rm eff}(\lambda)$ can be approximated by a simpler formula,

$$S_{\rm eff}(\lambda) = (S_1^{-1} + S_2^{-1}\exp(-\alpha(\lambda)d_p))^{-1}, \qquad (3)$$

where $S_1 = S_0$, $S_2 = S_p^{\min}$, and d_p is the near-surface layer thickness, in which S_{eff} varies. In this case, $d_p \approx \omega$. The results of approximation by formula (3) are also depicted in Fig. 1, and they evidently coincide well with the results obtained by expression (2).

In Fig. 2, the spectral dependences of the small-signal surface photovoltage normalized by the corresponding maximum values are depicted. They were recalculated for the same number of incident quanta with the use of expression (1), in which the dependence $S_{\text{eff}}(\lambda)$ described by formula (2) is taken into account. Curve *1* corresponds to the case of small S_{eff}, namely, $S_{\text{eff}} = 10^4$ cm/s = const. As follows from the figure, the short-wave recession, which is governed by the mechanism considered above, is absent in this case of the spectral dependence of the small-signal surface photovoltage, $V_f(\lambda)$.

The figure demonstrates that the smallest short-wave recession in $V_f(\lambda)$ is observed in the case where $S = 10^6$ cm/s (curve *2*) and the largest one at $S = 10^7$ cm/s (curve *4*). As we show below, the limiting cases and the cases where S_0 varies between the indicated values describe the experimental spectral dependences $V_f(\lambda)$ normalized by the photovoltage value in its maximum. However, in order to get convinced that it is the mechanism considered above, namely, the influence of SCR on the motion velocity of minority charge carriers, which is responsible for the short-wave recession of the photovoltage in experiment, it is necessary to be sure that not only the normalized spectral dependences $V_f(\lambda)$ but also the absolute values of $V_f(\lambda)$ calculated at the maximum point agree with the experiment in this case.

In Fig. 3, the dependences of the absolute values of $V_f(\lambda)$ calculated at the point of its maximum for a p-type silicon specimen on the magnitude of dimensionless equilibrium depleting band bending at the surface, y_s, are shown. They were obtained using formula (1) and taking expression (2) into account. The curves are parametrized by the value of S_0. The straight lines in the same figure designate the absolute values of $V_f(\lambda)$ at the maximum points, which are observed experimentally. A comparison between the experimental and calculated $V_f(\lambda)$-values shows that their correspondence occurs in the interval of surface band bendings $8 < y_s < 14$, with the specific y_s depending on the magnitude of S_0. In the case $S_0 \approx 10^4$ cm/s, the agreement takes place in the interval of band bendings $8 < y_s < 9.5$, whereas in

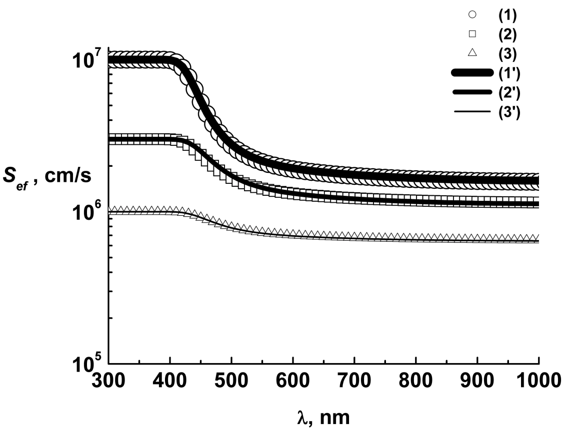

Fig. 1. (*a*) Dependences $S_{\text{eff}}(\lambda)$ calculated by formulas (2) (curves *1* to *3*) and (3) (curves *1′* to *3′*). The following parameters are used: $D = 30$ cm^2/s; $y_s = 15$; $S_0 = 10^6$ (curves *1* and *1′*), 3×10^6 (curves *2* and *2′*), and 10^7 cm/s (curves *3* and *3′*); $S_2 = 1.8\times10^6$ (*1′*), 1.85×10^6 (*2′*), and 1.9×10^6 cm/s (*3′*)

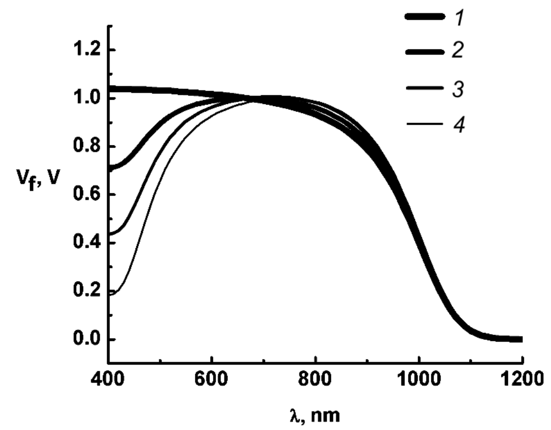

Fig. 2. Dependences $V_f(\lambda)$ calculated by formulas (1) and (2). The following parameters are used: $D = 30$ cm^2/s; $y_s = 15$; $p_0 = 10^{15}$ cm^{-3}; $L = 100$ μm; $S_0 = 10^4$ (*1*), 10^6 (*2*), 3×10^6 (*3*), and 10^7 cm/s (*4*); $\lambda_x = 670$ (*1* and *2*), 690 (*3*), and 760 nm (*4*)

the case $S_0 \approx 10^7$ cm/s, it occurs if $13 < y_s < 14$. By calculating the dimensionless values for the equilibrium band bendings of 0.22 and 0.26 V obtained at a temperature of 300 K, we get $y_s \approx 8.5$ and 10, respectively. Hence, as follows from the comparison between the experimental and theoretical values of small-signal surface photovoltage V_f, the quantity S_0 amounts to only about 10^2 cm/s in this case. This means that the mechanism governing the dependence $S_{\text{eff}}(\lambda)$, which was described above and is connected

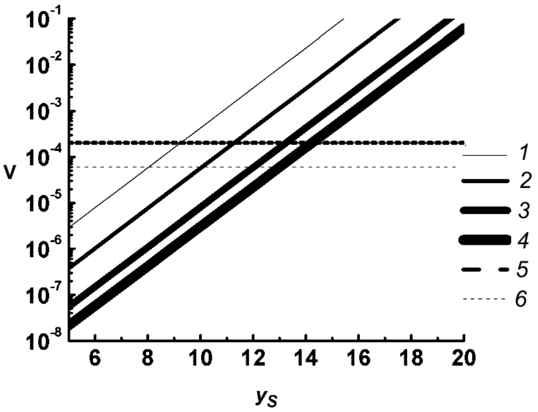

Fig. 3. Dependences of V_f on the equilibrium band bending y_s calculated by formulas (1) and (2). The following parameters are used: $\lambda = 700$ nm; $D = 30$ cm^2/s; $p_0 = 10^{15}$ cm^{-3}; $L = 100$ μm; $I = 10^{13}$ cm^{-2}s^{-1}; $S_0 = 10^4$ (*1*), 10^5 (*2*), 10^6 (*3*), and 10^7 cm/s (*4*). Lines *5* and *6* correspond to two experimental values of V_f

with a non-constant Fermi quasilevel for the minority charge carriers in the SCR, is not activated.

Therefore, for the explanation of the short-wave recession in the dependence $V_f(\lambda)$ for experimental specimens, other physical mechanisms have to be analyzed. In particular, they can be associated with short lifetimes of minority charge carriers in the near-surface layers of the silicon specimens under study. A similar scenario takes place, in particular, in silicon $p-n$-junctions with a high level of emitter doping. In this case, the bulk lifetime of charge carriers in the emitter is governed by the interband Auger recombination, so that it can be very short. In Introduction, we discussed the mechanism of short-wave recession in the surface photovoltage associated with the incomplete removal of the mechanically damaged layer. In this case, the recession may take place owing to a high concentration of recombination centers and, accordingly, a short lifetime in this layer. Experimentally, it is possible to obtain a strong reduction of the lifetime in the near-surface silicon layer by implanting an impurity, which would create a deep recombination level in silicon. In this case, the analysis of the short-wave recession in $V_f(\lambda)$ becomes an effective tool to study the details of near-surface recombination processes.

It should be noted that the two-layer theoretical model states that, in the near-surface semiconductor region, there exists a layer with a short lifetime of charge carriers, i.e. with an increased concentration of recombination centers, which is independent of the layer thickness. Therefore, the theoretical analysis of the dependence $S_{\text{eff}}(\lambda)$ and the spectral dependences of the surface photovoltage can be carried out identically for some cases of silicon $p-n$-junctions, e.g., mechanically damaged and implanted layers.

From the physical viewpoint, it is evident that the indicated dependences $S_{\text{eff}}(\lambda)$ can be observed when the surface recombination on the illuminated surface is restricted by the rate of diffusion-driven supply of minority charge carriers to the surface at arbitrary λ. In particular, as was shown in work [11], if there is a near-surface layer of the thickness x_j, in which the lifetime of minority charge carriers and their mobility are lower than the corresponding bulk values, the effective rate of surface recombination at $\alpha x_j \ll 1$ (light absorption in the bulk) is determined by the expression

$$S_2 = \frac{D_1}{L_1}\frac{S_0\frac{L_1}{D_1}\,\mathrm{ch}\left(\frac{x_j}{L_1}\right)+\mathrm{sh}\left(\frac{x_j}{L_1}\right)}{S_0\frac{L_1}{D_1}\,\mathrm{sh}\left(\frac{x_j}{L_1}\right)+\mathrm{ch}\left(\frac{x_j}{L_1}\right)}, \tag{4}$$

where D_1 and L_1 are the diffusion coefficient and the diffusion length, respectively, in the near-surface layer. In the case $\alpha x_j > 1$, the quantity α^{-1} plays the role of the effective near-surface layer thickness. Taking this circumstance into account, expression (2) transforms as follows:

$$S_{\text{ef}}(\lambda) = \frac{D_1}{L_1}\frac{S_0\frac{L_1}{D_1}\,\mathrm{ch}\left(\frac{1}{\alpha(\lambda)L_1}\right)+\mathrm{sh}\left(\frac{1}{\alpha(\lambda)L_1}\right)}{S_0\frac{L_1}{D_1}\,\mathrm{sh}\left(\frac{1}{\alpha(\lambda)L_1}\right)+\mathrm{ch}\left(\frac{1}{\alpha(\lambda)L_1}\right)}, \tag{5}$$

Formula (5) shows that, when α increases, i.e. the illumination wavelength λ decreases, the magnitude of $S_{\text{eff}}(\lambda)$ tends to S_0, and the restriction imposed by the diffusion-driven supply on the effective surface recombination rate becomes eliminated. At intermediate λ-values, the effective rate of surface recombination varies between the value determined by expression (4) and S_0. The quantity described by expression (5), identically to that described by formula (2), reflects a situation where the restriction of the effective surface recombination rate takes place owing to the restriction imposed on the rate of minority charge carrier supply to the surface. The difference between them consists in that the restriction is connected in this case with the velocity of motion of minority charge

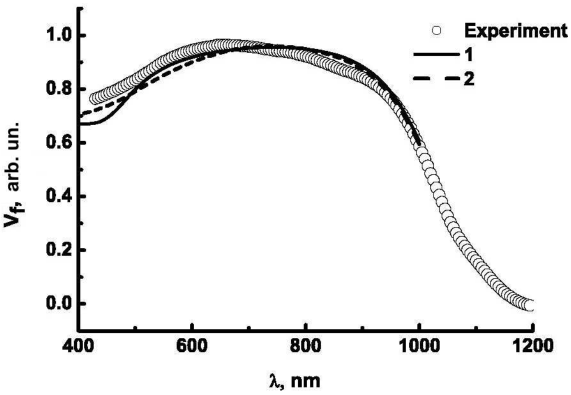

Fig. 4. Experimental (circles) and theoretical (curves) dependences $V_f(\lambda)$ normalized by the corresponding maximum values for the initial specimen. Curve *1* was calculated by formulas (1) and (3), and curve *2* by formulas (1) and (5). The following parameters are used: $D = 20$ cm^2/s; $L = 220$ μm; $\lambda_x = 800$ nm; $d_p = 1$ μm; $S_0 = 2 \times 10^3$ (*1*) and 4×10^3 cm/s (*2*); $S_2 = 2 \times 10^3$ cm/s; $D_1 = 1$ cm^2/s; and $L_1 = 4$ μm

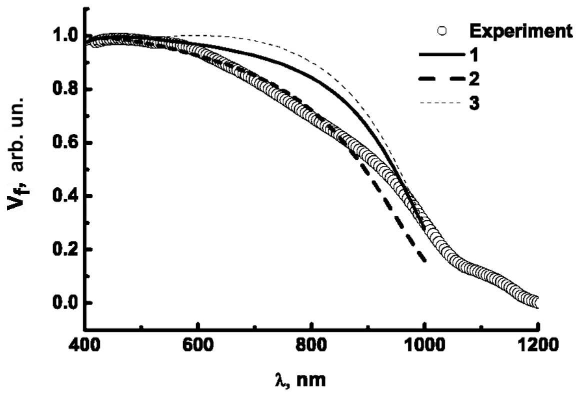

Fig. 5. Experimental (circles) and theoretical (curves) dependences $V_f(\lambda)$ normalized by the corresponding maximum values for the specimen annealed without a getter. Curve *1* was calculated by formulas (1) and (3), and curve *2* by formulas (1) and (5). The following parameters are used: $D = 20$ cm^2/s; $L = 60$ μm; $\lambda_x = 500$ nm; $d_p = 0.02$ μm; $S_0 = 3 \times 10^3$ cm/s; $S_2 = 3 \times 10^3$ cm/s; $D_1 = 1$ cm^2/s; and $L_1 = 4$ μm

carriers in the layer with a reduced lifetime, whereas, in the previous case, it occurs owing to the velocity of motion in the SCR.

It should be noted that expressions (3) and (5) – as well as expressions (2) and (3) – also give rise to similar dependences $S_{\rm eff}(\lambda)$. Moreover, for certain parameters, not only their dependences on the illumination wavelength λ, but also the limiting values in the long- and short-wave absorption intervals almost coincide.

Note that expression (3) provides information concerning the magnitudes of effective surface recombination rates $S_1 = S_0$ and S_2. At the same time, formula (5) additionally contains information on the diffusion length L and the diffusion coefficient D in the layer with a reduced lifetime τ_1. Whence, in particular, using the formula $\tau_1 = L_1^2/D_1 = (C_n N_t)^{-1}$, it is possible to determine the bulk lifetime in the near-surface layer and, therefore, the near-surface concentration of impurities, N_t, while identifying the nature of the latter [13].

4. Experimental Results and Their Discussion

In Figs. 4 to 6, the normalized spectral dependences of the small-signal photovoltage obtained for the initial specimens, specimens annealed in the argon atmosphere, and specimens, whose rear surface–after the specimens had been annealed–was covered with a getter layer of aluminum, are exhibited. From Fig. 4,

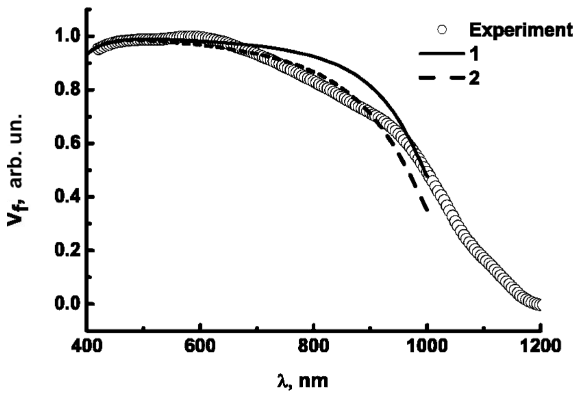

Fig. 6. Experimental (circles) and theoretical (curves) dependences $V_f(\lambda)$ normalized by the corresponding maximum values for the specimen annealed with a getter. Theoretical curves were calculated by formulas (1) and (3). The following parameters are used: $D = 20$ cm^2/s; $L = 140$ (*1*) and 70 μm (*2*); $\lambda_x = 600$ nm; $d_p = 0.03$ μm; $S_0 = 2.2 \times 10^3$ cm/s; and $S_2 = 2.3 \times 10^3$ cm/s

one can see that the normalized spectral dependences of the small-signal surface photovoltage demonstrate rather a weak recession. If one takes into account that the dimensionless equilibrium surface band bending for the initial specimens falls within the interval from 8.5 to 1, which corresponds to the absolute values of V_f ranging from 60 to 200 mV in the case where $S_0 \approx 10^4$ cm/s, it becomes clear that the mechanism giving rise to the dependence $S_{\rm eff}(\lambda)$ describing by

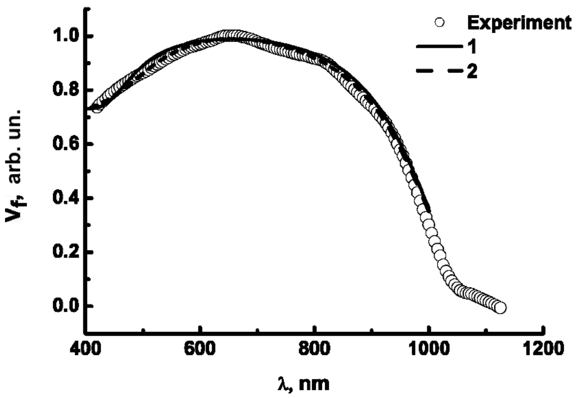

Fig. 7. Experimental (circles) and theoretical (curves) dependences $V_f(\lambda)$ normalized by the corresponding maximum values for the specimens implanted with iron to a dose of 2 μC/cm^2 and annealed without a getter. Curve *1* was calculated by formulas (1) and (3), and curve *2* by formulas (1) and (5). The following parameters are used: $D = 20$ cm^2/s; $L = 80$ μm; $\lambda_x = 700$ nm; $d_p = 0.7$ μm; $S_0 = 2 \times 10^4$ cm/s; $S_2 = 2 \times 10^4$ cm/s; $D_1 = 3$ cm^2/s; and $L_1 = 2.5$ μm

expression (2) is not realized. In this case, the short-wave recession of $V_f(\lambda)$ may probably be associated with a reduction of the bulk lifetime for excess charge carriers in a thin near-surface silicon layer, which may be the remnants of the mechanically damaged layer, which had not been etched completely. Note that the application of expressions (3) and (5) in this case allows the theoretical and experimental dependences to be put in accordance. The corresponding thickness of the damaged layer was about 1 μm, and the diffusion length in this layer turned out considerably reduced with respect to the bulk value and amounted to 4 μm. Such a strong decrease is related to a reduction in not only the bulk lifetime, but also in the mobility of minority charge carriers, which occurs owing to the amorphization (defectiveness) of the damaged layer.

After the initial specimens had been annealed in the argon atmosphere for 30 min at a temperature of 750 °C, the shape of spectral dependence $V_f(\lambda)$ changed substantially. The results obtained after two regimes of annealing are depicted in Figs. 5 and 6. The difference between those cases consists in that, in the latter one, the rear surfaces of initial semiconductor specimens before the annealing were covered by an aluminum layer. During the annealing, this layer acted as an effective getter. From Fig. 5, one can see that the short-wave recession in $V_f(\lambda)$ is practically absent for the annealed aluminum-free specimen, which testifies, first of all, to a strong reduction of the damaged layer thickness. Really, after the annealing, the value of this parameter obtained by fitting the theoretical dependence (3) to experimental values decreased from about 1 to 0.02 μm. The rate of surface recombination amounted to 3×10^3 cm/s at that, i.e. it is rather low. However, the bulk values of diffusion length in the specimens were subjected to largest variations during their annealing. The magnitude of L drastically diminished. In the interval of short enough λ (500 nm $< \lambda <$ 900 nm), the shape of dependence $V_f(\lambda)$ considerably transformed. In this region, the theoretical curves approximated the experimental ones at $L \approx 30$ μm, whereas, at $\lambda > 900$ nm, the fitting brought about a much larger value, $L \approx 60$ μm. Before the annealing, the initial specimens had $L = 220$ μm. Therefore, it has to be recognized that the annealing of specimens at $T = 750$ °C resulted in a very strong reduction of the diffusion length. For the annealed specimens with aluminum on the rear surface, the diffusion length amounted to 70 μm within the interval 500 nm $< \lambda <$ 900 nm and to 140 μm at $\lambda = 900$ nm. Hence, the gettering manifested itself rather strongly in this case. The short-wave recession of the photovoltage increased at that, but it was not a result of the growth of the surface recombination rate. In this case, the thickness of the defect layer increased a little (to 0.03 μm).

The influence of a thermal treatment on the recombination characteristics of silicon was studied earlier in detail in a number of works (see [12]). In particular, three characteristic temperature sections were revealed: 200–500 °C, where an increase of the lifetime was observed; 500–800 °C, where the lifetime decreased more than one order of magnitude; and 850–1100 °C, where the annealing of recombination centers was observed again, and the lifetime substantially increased. Those experiments were carried out without gettering treatments. Therefore, it is natural that the results obtained with the use of getters differ from those obtained earlier (see work [13]).

In Figs. 7 and 8, the spectral dependences $V_f(\lambda)$ for annealed specimens without and with, respectively, aluminum on the rear surface and implanted with iron ions to a dose of 2 μC/cm^2 are depicted. It is known that iron after the annealing creates deep centers which are recombination levels [12, 13]. As is seen from those figures, as the implantation increases,

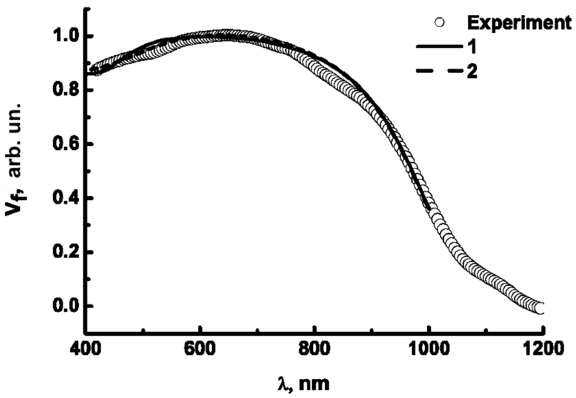

Fig. 8. Experimental (circles) and theoretical (curves) dependences $V_f(\lambda)$ normalized by the corresponding maximum values for the specimens implanted with iron to a dose of 2 μC/cm^2 and annealed with a getter. Curve *1* was calculated by formulas (1) and (3), and curve *2* by formulas (1) and (5). The following parameters are used: $D = 20$ cm^2/s; $L = 80$ μm; $\lambda_x = 700$ nm; $d_p = 0.6$ μm; $S_0 = 5 \times 10^4$ cm/s; $S_2 = 1.2 \times 10^4$ cm/s; $D_1 = 1$ cm^2/s; and $L_1 = 2.8$ μm

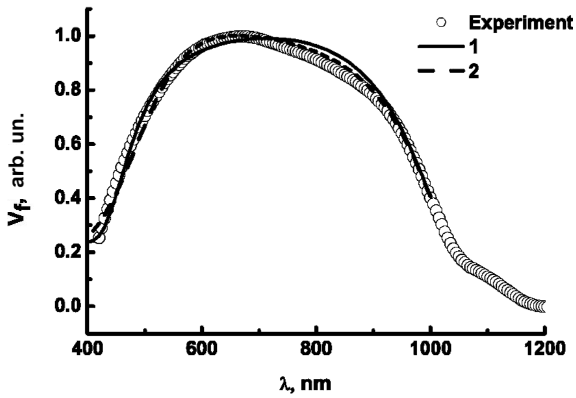

Fig. 9. Experimental (circles) and theoretical (curves) dependences $V_f(\lambda)$ normalized by the corresponding maximum values for the specimens implanted with iron to a dose of 18 μC/cm^2 and annealed without a getter. Curve *1* was calculated by formulas (1) and (3), and curve *2* by formulas (1) and (5). The following parameters are used: $D = 20$ cm^2/s; $L = 100$ μm; $\lambda_x = 700$ nm; $d_p = 0.6$ μm; $S_0 = 4 \times 10^4$ (*1*) and 2×10^4 cm/s (*2*); $S_2 = 8 \times 10^3$ cm/s; $D_1 = 1$ cm^2/s; and $L_1 = 1.7$ μm

the short-wave recession in $V_f(\lambda)$ becomes stronger in comparison with that in only annealed specimens. A comparison of the theory with the experiment gives a damaged layer thickness of 0.5 μm in this case. If one takes into account that, first, the maximum in the distribution profile of implanted iron both before and after the annealing is located at a distance of 0.2 μm and, second, the applied model is approximate (the assumption of the uniformity of a recombination level distribution, which was used at calculations, resulted in an increase of the damaged layer thickness in comparison with a true profile of the iron distribution), a value of 0.5 μm obtained for the damaged layer thickness turned out rather close to the experimental one. Attention is also drawn by the circumstance that, in this case, the effect of the Fe impurity gettering from the specimen bulk turned out inefficient. At the same time, the rates of surface recombination increased rather substantially in this case in comparison with those for the initial specimens and amounted to 2×10^4 cm/s.

Figures 9 and 10 demonstrate the spectral dependences $V_f(\lambda)$ for the annealed specimens without and with, respectively, aluminum on the rear surface and implanted with iron ions to a high dose of 18 μC/cm^2 . As one can see from those figures, the short-wave recession in this case becomes even stronger in comparison with the case where the dose of implanted iron was 2 μC/cm^2. A comparison of theoretical and experimental data shows that the thickness of the damaged layer grew in this case to 0.7 μm, and the effective rate of surface recombination to 4×10^4 cm/s. The diffusion length in the damaged layer diminished at that to 1.7–2 μm in comparison with the previous case where L was equal to 2.5–2.8 μm.

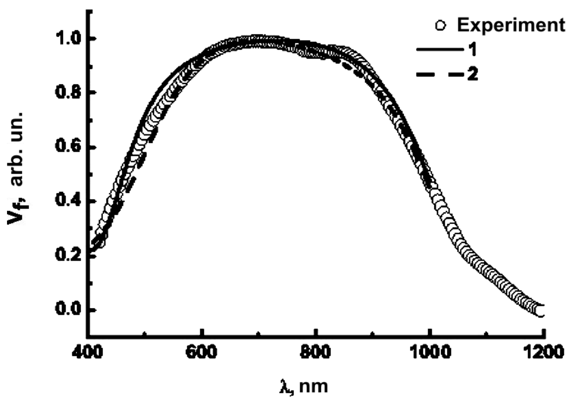

Fig. 10. Experimental (circles) and theoretical (curves) dependences $V_f(\lambda)$ normalized by the corresponding maximum values for the specimens implanted with iron to a dose of 18 μC/cm^2 and annealed with a getter. Curve *1* was calculated by formulas (1) and (3), and curve *2* by formulas (1) and (5). The following parameters are used: $D = 20$ cm^2/s; $L = 120$ μm; $\lambda_x = 700$ nm; $d_p = 0.6$ μm; $S_0 = 5 \times 10^4$ cm/s; $S_2 = 1 \times 10^4$ cm/s; $D_1 = 2$ cm^2/s; and $L_1 = 2.1$ μm

5. Conclusions

To summarize, the studies of the spectral dependence $V_f(\lambda)$ in the short-wave spectral interval allows a detailed information on the changes in recombination properties that occur on the surface and in the photosensitive silicon bulk at various technological treatments to be obtained experimentally with the use of a nondestructive technique. In particular, it is shown for the first time that the formation of a mechanically damaged near-surface layer owing to the implantation of iron ions gives rise to a drastic reduction of the bulk diffusion length (i.e. the bulk lifetime) in the implanted layer and to a growth of the effective surface recombination rate on the illuminated surface. Hence, the proposed nondestructive method allows the bulk and surface recombination parameters to be determined separately in a wide range of their variation.

1. W. Gartner, Phys. Rev. **105**, 823 (1997).
2. V.A. Zuev and V.G. Litovchenko, Phys. Status Solidi A **16**, 175 (1966).
3. V.A. Zuev and V.G. Litovchenko, Surf. Sci. **32**, 365 (1972).
4. L. Kronik and Y. Shapira, Surf. Sci. Rep. **37**, 1 (1999).
5. A.P. Gorban', V.P. Kostylyov, V.G. Litovchenko, A.V. Sachenko, and O.V. Snitko, Ukr. Fiz. Zh. **34**, 404 (1989).
6. A.P. Gorban', V.P. Kostylyov, A.V. Sachenko, A.A. Serba, and V.V. Chernenko, Optoelektron. Poluprovodn. Tekhn. **37**, 61 (2002).
7. A.P. Gorban', V.P. Kostylyov, A.V. Sachenko, O.A. Serba, I.O. Sokolovskyi, and V.V. Chernenko, Ukr. Fiz. Zh. **55**, 784 (2010).
8. V.V. Antoshchuk, V.V. Milenin, V.E. Primachenko, and O.V. Snitko, Fiz. Tekh. Poluprovodn. **11**, 2002 (1977).
9. V.G. Litovchenko and A.P. Gorban', *Fundamentals of Microelectronic Metal–Insulator–Semiconductor Systems* (Naukova Dumka, Kyiv, 1978) (in Russian).
10. A.V. Sachenko and O.V. Snitko, *Photo-Effects in Near-Surface Layers of Semiconductors* (Naukova Dumka, Kyiv, 1984) (in Russian).
11. A.L. Fahrenbruch and R.H. Bube, *Fundamentals of Solar Cells: Photovoltaic Solar Energy Conversion* (Academic Press, New York, 1983).
12. K.D. Glinchuk and N.M. Litovchenko, Poluprovodn. Tekhn. Mikroelektron. **28**, 4 (1978).
13. V.G. Litovchenko, V.M. Naseka, and A.A. Evtukh, Ukr. J. Phys. **57**, 73 (2012).

Received 19.09.12.
Translated from Ukrainian by O.I. Voitenko

А.В. Саченко, В.П. Костильов,
В.Г. Литовченко, В.Г. Попов, Б.М. Романюк,
В.В. Черненко, В.М. Насєка, Т.В. Слусар,
С.І. Кирилова, Ф.Ф. Комаров

РЕКОМБІНАЦІЙНІ ХАРАКТЕРИСТИКИ ПЛАСТИН МОНОКРИСТАЛІЧНОГО КРЕМНІЮ З ПРИПОВЕРХНЕВИМ ПОРУШЕНИМ ШАРОМ

Р е з ю м е

Експериментально та теоретично досліджено спектральні залежності малосигнальної конденсаторної фото-ерс $V_f(\lambda)$ з ділянкою короткохвильового спаду. Показано, що в короткохвильовій області спектра залежності $V_f(\lambda)$ дозволяють отримати з використанням експериментально неруйнівного методу важливу інформацію про зміну рекомбінаційних властивостей поверхні та об'єму фоточутливого кремнієвого матеріалу. Встановлено, зокрема, що створення порушеного приповерхневого шару за рахунок імплантації заліза приводить як до сильного зменшення об'ємної довжини дифузії (тобто часу життя) в імплантованому шарі, так і до зростання ефективної швидкості поверхневої рекомбінації на освітлюваній поверхні.